

Study on Erosion Results of Temporary Venting Device in Shale Gas Pipeline Station

Yong Chen^{1,2,*}, Zheng Zhang¹, Dongying Meng³, Jinjin Tan⁴

¹School of Mechanical and Electrical Engineering, Southwest Petroleum University, Chengdu 610500, China

²Oil and Gas Equipment Technology Sharing and Service Platform of Sichuan Province, Chengdu, China

³Gas Transmission Management Department of PetroChina Southwest Oil and Gasfield Company, Chengdu, China

⁴Chengdu HOLY Industry & Commerce CORPLtd. (Group), Chengdu, China

*Corresponding author: swpucy1412@163.com

Abstract: A temporary venting device for shale gas pipeline station is designed. After one year of adhibition, there are pits in the elbow of the venting pipe, which is presumed to be caused by the erosion of the elbow by untreated shale gas in the gas collector. The erosion model is simplified. The sand is set as the discrete phase, and the gas and liquid are set as the continuous phase. Based on the VOF model and the DPM discrete phase model of multiphase flow, the erosion rate of U-shaped pipe is studied by ANSYS Fluent. The internal flow field of multiphase flow in the pipe is studied. The influence of solid particle velocity, mass flow, particle diameter, curvature-to-diameter rate and pipe diameter on the erosion rate of the elbow is studied by using the control variable method. The influence of various factors on the erosion rate is analyzed by grey correlation analysis. It provides a basis for reducing the erosion rate of U-shaped pipeline and prolonging the service life of pipeline.

Keywords: FLUENT; CFD; Shale gas; Erosion rate; Grey Correlation analysis; Pipeline failure analysis.

1. Introduction

The " West-East Gas Transmission " and " Sichuan-East Gas Transmission " projects have benefited nearly 500 million people in western China, the Yangtze River Delta, the Pearl River Delta and central China[1]. After a temporary venting device for a shale gas transmission station has been in service for a period of time, there are pits inside the elbow, which may be the erosion of the elbow caused by untreated shale gas. It is found that untreated shale gas often contains solid particles such as sand. Sudden changes in the diameter and direction of the pipeline will cause sudden changes in the rate and direction of the fluid flow, which is easy to cause erosion damage to the device.

Experimental tests and CFD simulations were used to study the erosion of continuous pipelines. The mechanism of erosion process was discussed. The effects of flow rate, solid particle size and density, fluid viscosity, particle acceleration pressure and retention distance on erosion rate and particle impact rate were studied[2~4]. The failure analysis of the macroscopic characteristics and SEM of the high pressure elbow is carried out, and the failure reason and mechanism are obtained. The erosion wear test bench and experimental system were further established, and the main parameters affecting erosion wear were extracted[5]. Costa et al.[6] used an additional CFD method to optimize the geometry of typical pipe elbows, and used ANSYS Fluent CFD software and discrete solvers to guide pipe type correction in a step-by-step manner to reduce pipeline pressure drop. Finally, the influence of optimized shape configuration on the prediction of three commonly used erosion models was discussed. In the study of 90° bend pipe, considering the solid-liquid interaction, V.Singh et al.[4] used the continuous / fluid phase flow $k-\epsilon$ turbulence model to track the solid particles, evaluated the erosion rate, and studied the effects of velocity, particle size and concentration on erosion. Jashanpreet Singh[7] used the discrete phase erosion wear model and

solved the control equation by Euler-Lagrange format to predict the erosion of 90° elbow. The standard $k-\epsilon$ turbulence scheme was used to study the particle tracking of bottom ash slurry flow. The variation of erosion wear with velocity distribution and turbulence intensity was studied. Mikilkumar B.Gandhi et al.[8] used Eulerian-Lagrangian method to analyze the continuous phase and particle tracking of coal particles. The obtained particle velocity and trajectory data have been used to predict the erosion degree of the selected area of the boiler. Waclaw et al.[9] used Fluent numerical simulation software to study the influence of steam and air convection on boiler erosion through mass loss measurement and numerical calculation. Based on the basic theory of solid-liquid two-phase flow and erosion model, the effects of support particle size, particle mass flow rate, half cone angle of pump valve, inlet radius of valve seat hole and lift of valve plate on erosion characteristics of pump valve were studied by CFD method[10]. The discrete phase model was used to simulate the erosion failure process of sand particles in gas-liquid mixing. The effects of fluid velocity, sand volume fraction, liquid volume fraction and opening height on the erosion rate under three-phase flow were analyzed[11]. Kun Ding and M. Amara et al.[12, 13] used Fluent software and numerical simulation method to study the erosion wear of tools with different media containing different particle sizes. Using Fluent, based on four erosion models, the discrete phase model was used to simulate the influence of different particle sizes on the erosion rate, and the maximum erosion wear rate near the outlet of the curve was obtained[14]. Based on CFD-DEM, considering the interaction between multiphase flow and boundary, the erosion of liquid-particle two-phase flow at the elbow joint was simulated[15].

In summary, ANSYS Fluent is mainly used to study the erosion at home and abroad. The classical erosion model is used. The conventional variables include fluid velocity, particle size, pipe bending diameter ratio, discrete phase particle mass flow rate etc. The pipeline erosion rate under

different parameter conditions is calculated by changing the parameters. However, there are few studies on the simultaneous existence of gas-liquid-solid three-phase in the current erosion research. However, gas-liquid-solid may exist at the same time under most actual working conditions. Therefore, based on this, according to the venting device model, from the influence of multiple factors on the erosion rate, the influence of various factors on the erosion rate is studied, and the influence degree of various factors on the

erosion rate is analyzed.

As shown in figure 1, the external morphology of the elbow of the temporary venting device, and the external morphology of the elbow of the temporary venting device, and the internal erosion situation of the pipeline in Figure 2 has been marked in the figure, and it can be seen that after a period of use, there is an obvious erosion pit at the elbow, and the wall thickness of the elbow is thinned, which may affect the working life of the elbow.



Figure 1. Venting pipe elbow



Figure 2. Erosion pits inside the vent pipe elbow

2. Geometric Model of Venting Pipeline

As shown in figure 3, the working principle of the venting device is designed. The arc plate of the assembled sealing ring is fixed on the pipeline through the fastening device. During

the first assembly, the valve and the arc plate connecting pipe are connected by thread (for rapid installation, the subsequent use is no longer disassembled). The valve is also connected with the fast joint of the buckle type through the thread, the fast joint is connected with the venting pipe, and the venting pipe is fixed with the bracket.

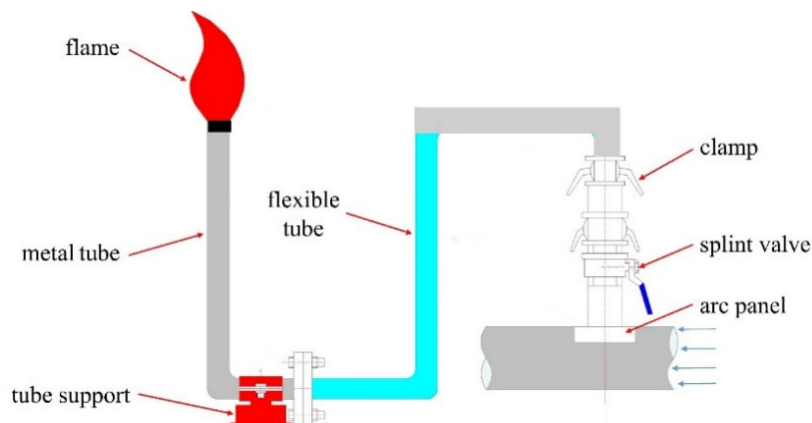


Figure 3. Working principle of venting device

3. Erosion Numerical Analysis of Vent Pipe Elbow

3.1. Basic Condition Settings

The discrete phase DPM model is used to calculate the gas-liquid-solid three-phase steady state at the elbow of the pipeline. The Realizable $k-\varepsilon$ turbulence model and the DPM model are used to track the particle trajectory. The continuous phase fluid is a mixture of gas-phase methane and liquid water. Methane uses the default parameters in the FLUENT material library, with a density of 0.6679 kg/m^3 and a viscosity of $1.087 \times 10^{-3} \text{ kg/(m}\cdot\text{s)}$. The liquid water density is 998.2 kg/m^3 and the viscosity is $0.001003 \text{ kg/(m}\cdot\text{s)}$. The turbulence intensity is determined to be 5%, and the hydraulic diameter (pipe diameter) is 219 mm. The discrete phase is released from the inlet through the surface type injection source, and the velocity inlet is selected. The velocity is equal to the continuous phase velocity, the particle diameter is $1 \times 10^{-4} \text{ m}$, and the particle mass flow rate is 1 kg/s . The outlet boundary condition is set as 'outflow', and the particle phase boundary condition is set as 'escape'. The general erosion model is selected for the wall erosion model, and the discrete model condition is 'reflect'. The normal rebound coefficient and tangential rebound coefficient of the discrete phase are determined by formula (1) and formula (2) respectively. The impact angle is bilinear input [16].

$$e_n = 0.993 - 0.037\theta + 4.75 \times 10^{-4}\theta^2 - 2.61 \times 10^{-6}\theta^3 \quad (1)$$

$$e_t = 0.988 - 0.0209\theta + 6.43 \times 10^{-4}\theta^2 - 3.56 \times 10^{-6}\theta^3 \quad (2)$$

3.2. Calculation settings

In the calculation of circulation, due to the large velocity difference between gas and liquid, the combined use of Euler-Euler hybrid model and VOF model can solve the error caused by only using VOF model, and Multi-Fluid VOF model is used for calculation. By calculating the governing equations of each phase in the mixed phase, the dynamic evolution and transient characteristics of each component in the mixing process can be accurately simulated. The continuity equation and momentum equation of the fluid are respectively (3) and (4) [17-20]:

$$\frac{\partial \varepsilon_f}{\partial t} + \nabla \cdot (\varepsilon_f u) = 0 \quad (3)$$

$$\frac{\partial (\rho_f \varepsilon_f u)}{\partial t} + \nabla \cdot (\rho_f \varepsilon_f u^2) = -\varepsilon_f \nabla p + \nabla \cdot \{ \varepsilon_f [\mu (\nabla u + \nabla u^T) + \rho_f g + F_{st}] \} + F_{pf} \quad (4)$$

Among them:

ρ_f is the fluid density; ε_f is the porosity; u is the fluid velocity; p is pressure, Pa; μ is the viscosity of the mixture, $\text{N}\cdot\text{s/m}^2$; F_{pf} the reaction force of the interaction between particles of the fluid; F_{st} is the surface tension of the free surface.

3.3. Erosion rate calculation

Solid particles are regarded as discrete phases, so the Euler-Lagrange method (5) is selected for the calculation of gas-liquid-solid three-phase. The erosion wear model is [21]:

$$R_{erosion} = \sum_{p=1}^{N_{particle}} \frac{m_p C(d_p) f(\alpha) V_p^{b(V_p)}}{A_{face}} \quad (5)$$

Among them:

m_p is the mass flow rate of particles; $C(d_p)$ is the particle size function; $f(\alpha)$ is the impact angle function; V_p is the relative velocity of particles impacting the wall; $b(V_p)$ is a function of this relative velocity; A_{face} is the surface area of the calculation unit. The piecewise linear input impact angle function is selected in the finite element calculation. The input angle and the corresponding value are shown in Table 1.

Table 1. Impact angle

Position	Angle/ $^\circ$	$f(\alpha)$
1	0	0
2	20	0.8
3	30	1
4	45	0.5
5	90	0.4

3.4. Mesh division

The finite element software is used to mesh the pipeline. For example, figure 4 is a mesh model. In the division of the mesh, watertight geometry is selected, and the size function type is face size; the maximum size of the generated surface mesh is 0.005 m, and the minimum size is 0.0005 m, as shown in figure 4-a; in order to accurately obtain the effect of the flow field near the wall, the boundary layer is added. The boundary layer has a total of 5 layers, and the growth rate is 1.2; finally, the volume grid is generated on the basis of the surface grid, and the grid type is 'poy-hexcore'.

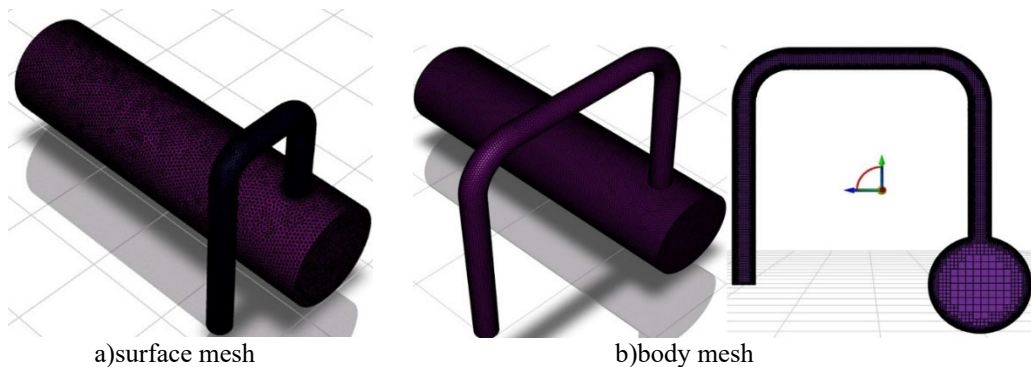


Figure 4. Mesh division

3.5. Mesh independence verification

The pipe diameter is set to 0.05m, the multiphase flow velocity is 10m/s, the particle mass flow rate is 1kg/s, the particle density is 2650kg/m³, and the particle size is 0.0001m. Draw figure 5 according to the results. When the number of grids increases from 147091 to 413229, the maximum erosion

rate increases. After the number of grids reaches 656586, the maximum erosion rate almost no longer increases. It is considered that after the number of grids, the increase in the number of grids has limited improvement in the calculation accuracy and reaches the calculation threshold of grid independence.

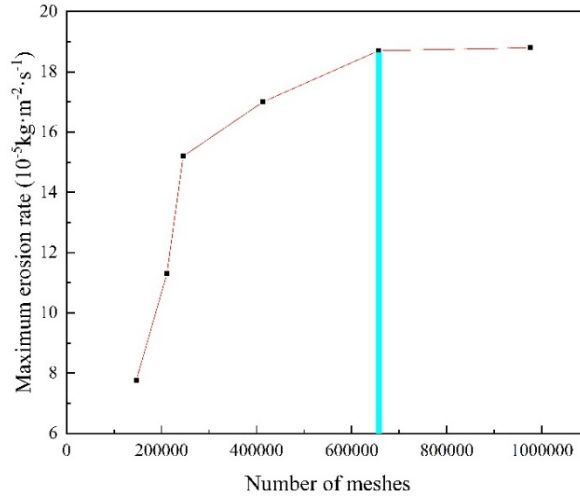


Figure 5. Mesh independence verification

4. Analysis of Erosion Results

4.1. Internal flow field analysis

According to the actual working conditions, the pipe parameters were selected for flow field analysis. Figure 6 describes the velocity contours of two-phase flow and gas-liquid-solid three-phase flow with liquid volume fraction of 10% under V=5m/s, particle size of 100 μm and 0.1kg/s

respectively. As shown in figure 6-a, the flow velocity in the pipe is almost unchanged; under the three-phase flow condition, the velocity of the inner arc and the outer arc at the elbow is obviously different, that is, the velocity at the inner arc is large and the velocity at the outer arc is small, as shown in figure 6-b. This is due to the centrifugal effect at the bend and the secondary flow caused by the increase of turbulence level in the bend region.

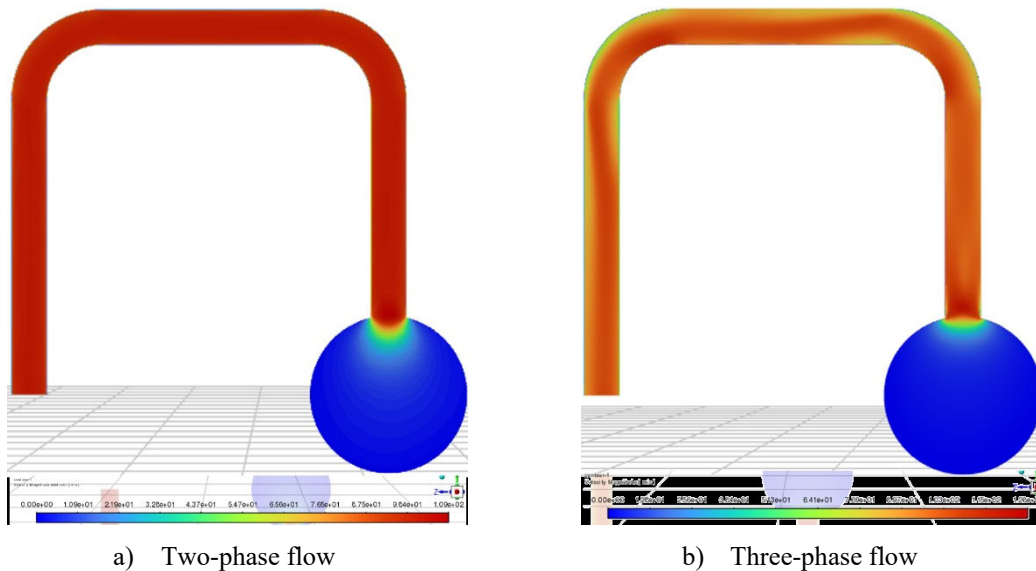


Figure 6. Comparison of flow velocity

Under the same tube parameters, the turbulence intensity of two-phase flow and three-phase flow tube with 10% liquid volume fraction is analyzed, as shown in figure 7. As shown in figure 7-a, the turbulence intensity at the elbow is not obvious under the two-phase condition, and there is a large

turbulence at 45°. Figure 7-b shows that there are more large turbulence in the three-phase flow condition. The turbulence intensity increases from 0° to 90° in the figure, and the turbulence intensity on the outer ring is greater than that on the inner ring on the same section.

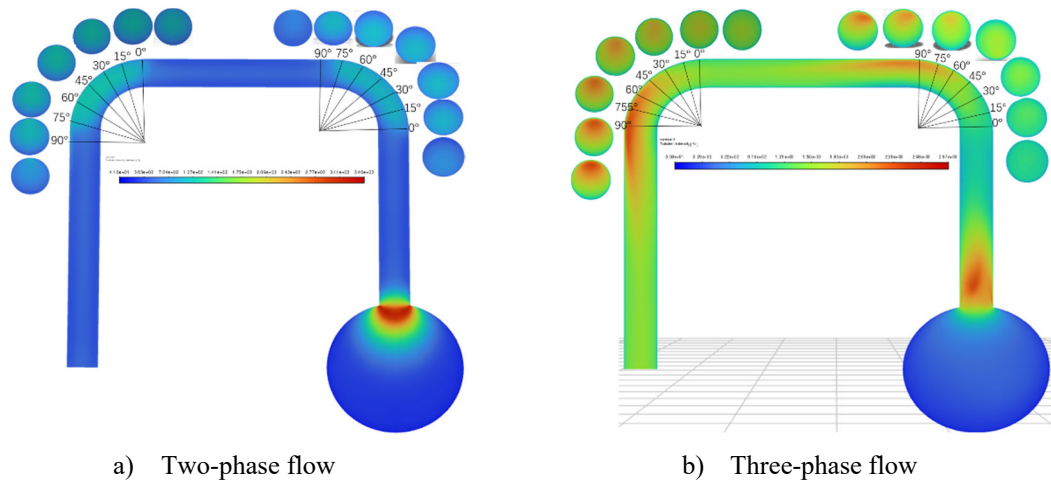


Figure 7. Turbulence intensity analysis

The results of pressure analysis in the tube show that there is almost no pressure difference on the same section under the condition of two-phase flow. In the case of three-phase flow,

the pressure at the elbow is always greater than the outer arc, as shown in figure 8.

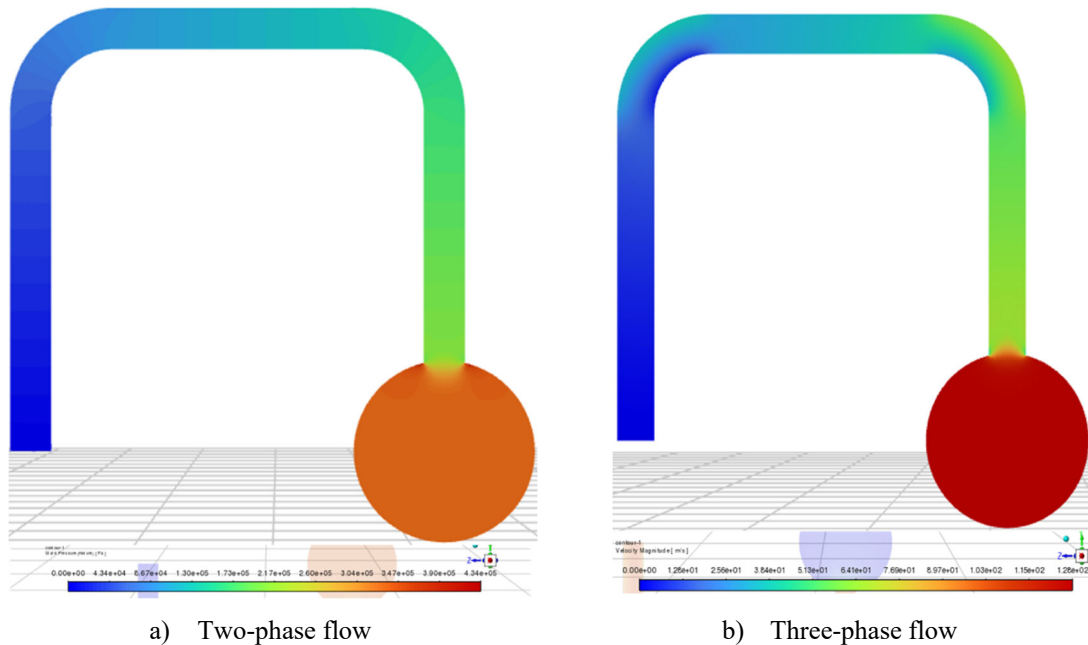


Figure 8. Pressure comparison

4.2. Analysis of solid particle velocity erosion results

The diameter of the pipe is set to a fixed value of 219 mm, and the influence of the incident velocity of solid particles on the erosion rate of the pipe is studied. The solid particle diameter is $100\mu\text{m}$, the bending diameter ratio is 1, the mass flow rate is 0.05 kg/s, and the incident velocity is (1m/s, 2m/s, 4m/s, 6m/s, 8m/s, 10m/s, 12m/s, 14m/s). When calculating the influence of incident velocity on erosion rate, the above velocity parameters are changed in turn to obtain the calculation results of erosion rate.

As shown in figure 9, the maximum erosion rate cloud

diagram of the pipeline at different flow rates. It can be seen from the figure that pipeline erosion mainly occurs at the elbow of the pipeline. Through the particle trajectory, it is found that the above reasons are mainly that the solid particles with kinetic energy collide directly with the pipe elbow and rebound. At the same time, because most of the solid particles collide with the flow direction of the U-shaped tube, the erosion phenomenon mainly occurs in the direction of the flow. By comparing the erosion rate at different flow rates, it is found that with the increase of flow rate, the erosion at the U-shaped pipe bend is more and more concentrated, and the erosion rate is more and more large.

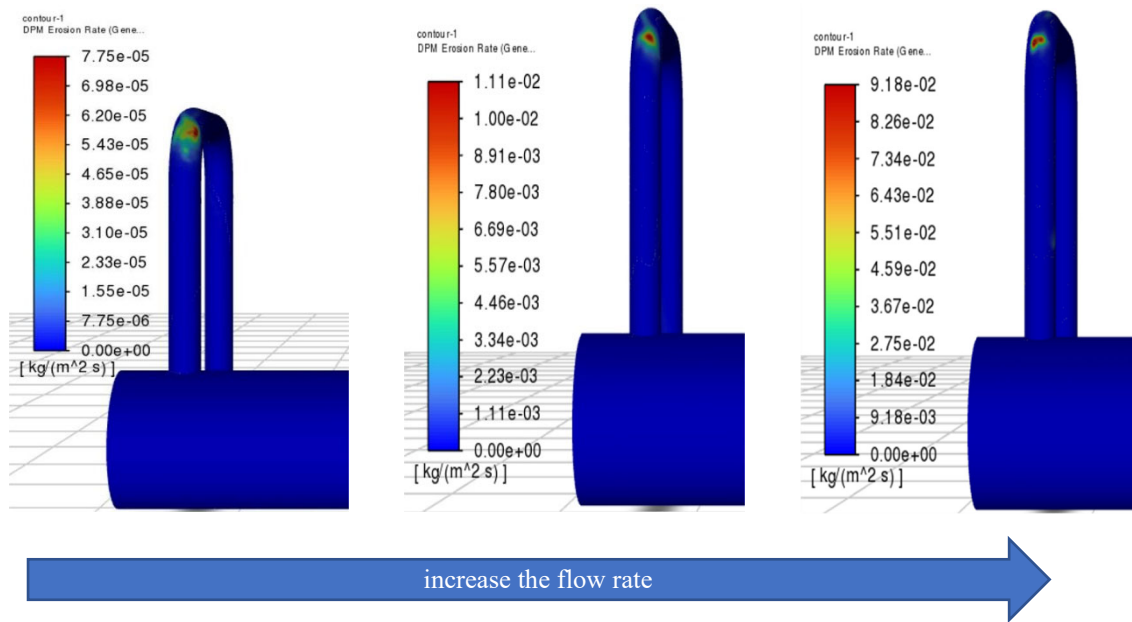


Figure 9. The maximum erosion rate cloud diagram of pipeline at different flow rates

Figure 10 shows the variation curve of the maximum erosion rate of the pipeline under different incident velocities of solid particles. It can be seen from the curve that the maximum erosion rate increases with the increase of velocity, which indicates that the flow rate has a great influence on the erosion rate. When other conditions remain unchanged, the greater the flow rate, the greater the kinetic energy obtained by the solid particles, the greater the relative velocity when colliding with the pipe wall, and the greater the erosion rate. Figure 11 shows the curve of the maximum erosion rate under two-phase flow and three-phase flow. Under the premise of other conditions unchanged, the erosion rate of the three-phase flow is greater than the maximum erosion rate in the gas-solid two-phase state. This also shows that the fluid containing solid particles has a stronger erosion effect on the pipe wall.

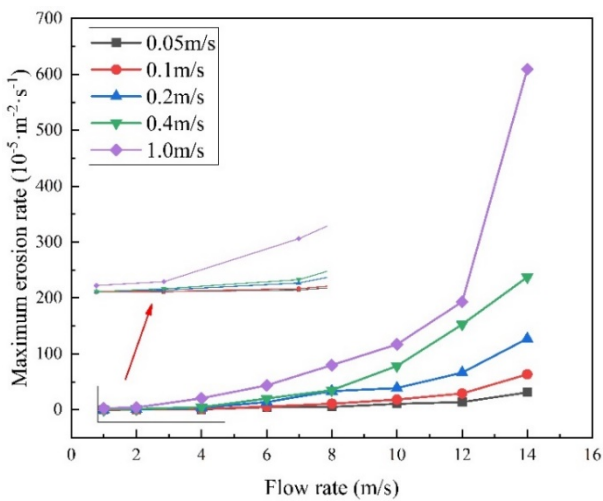


Figure 10. The curve of maximum erosion rate changing with flow velocity

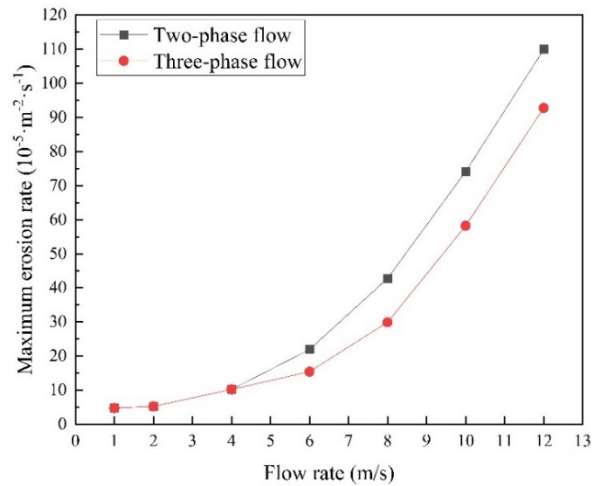


Figure 11. Comparison of maximum erosion rate of two-phase flow and three-phase flow

4.3. Analysis of the influence of mass flow

The mass flow rate (0.05kg/s, 0.1kg/s, 0.2kg/s, 0.4kg/s, 1.0kg/s) was changed in turn, and other parameters were set as constants: the pipe diameter was 219 mm, the solid particle diameter was $100\mu\text{m}$, the bending diameter ratio was 1, and the incident velocity was 10m/s.

As shown in figure 12, at the same flow rate, with the increase of particle mass flow rate, the range of erosion marks on the pipe wall gradually expands, and the maximum erosion rate increases accordingly. This is because as the number of particles per unit volume increases, the number of collisions between the particle phase and the U-shaped tube increases; at the same time, because of the randomness of the movement of solid particles, the collision range of solid particles here is larger, forming a larger erosion trace; due to the repeatability of the particle phase movement, more solid particles collide multiple times in the pipeline, thus forming deeper erosion pits and increasing the erosion rate.

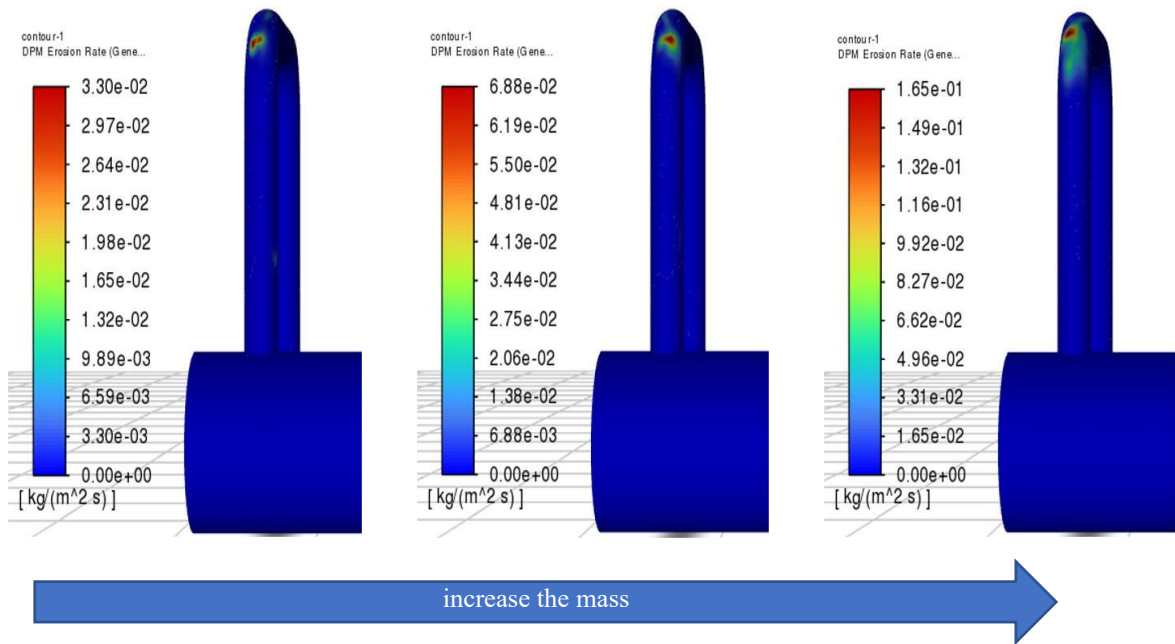


Figure 12. The maximum erosion rate cloud diagram under different mass flow rates

Figure 13 shows the influence of mass flow rate on erosion rate. It can be seen from the figure that the erosion rate increases with the increase of mass flow rate. This is because with the increase of mass flow rate, the fluid mass passing

through the effective section of the pipeline in unit time increases, the number of particles carried by the fluid increases, more particles will repeatedly collide with the wall surface, and the erosion rate of the bend increases.

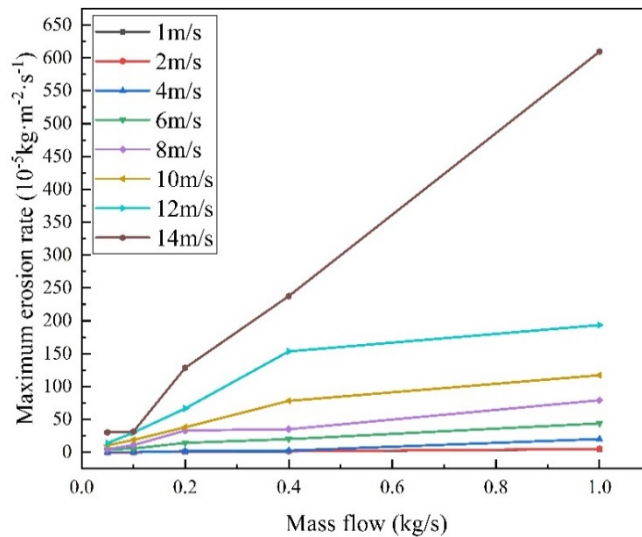


Figure 13. Effect of mass flow rate on erosion rate

4.4. Effect of particle diameter on erosion rate

The effect of particle diameter on the maximum erosion rate was studied. The pipe is directly fixed to 219 mm, the bending diameter ratio is 1, the incident velocity is 10 m/s, and the mass flow rate is 0.2 kg/s. The particle diameters were 50 μ m, 100 μ m, 150 μ m, 200 μ m, 250 μ m, 300 μ m, 500 μ m and 1000 μ m respectively. By changing the above particle size parameters in turn, the influence on the erosion rate of the pipeline is calculated, and the results are shown in figure 14.

It can be seen from figure 14 that the smaller the particle diameter, the greater the erosion rate of the pipeline. This is

because when the sand diameter is small, the mass flow rate is constant, and the smaller the particle diameter, the more sand particles will collide with the pipe wall. With the increase of particle size, the erosion rate shows a decreasing trend as a whole, and the erosion marks left on the elbow also increase with the increase of particle size. By analyzing the above erosion phenomenon, it can be seen that with the increase of particle size and the contact surface of the pipe wall, the impact force decreases when the particles with the same momentum collide with the pipe wall every time, the erosion rate decreases, and the erosion surface increases.

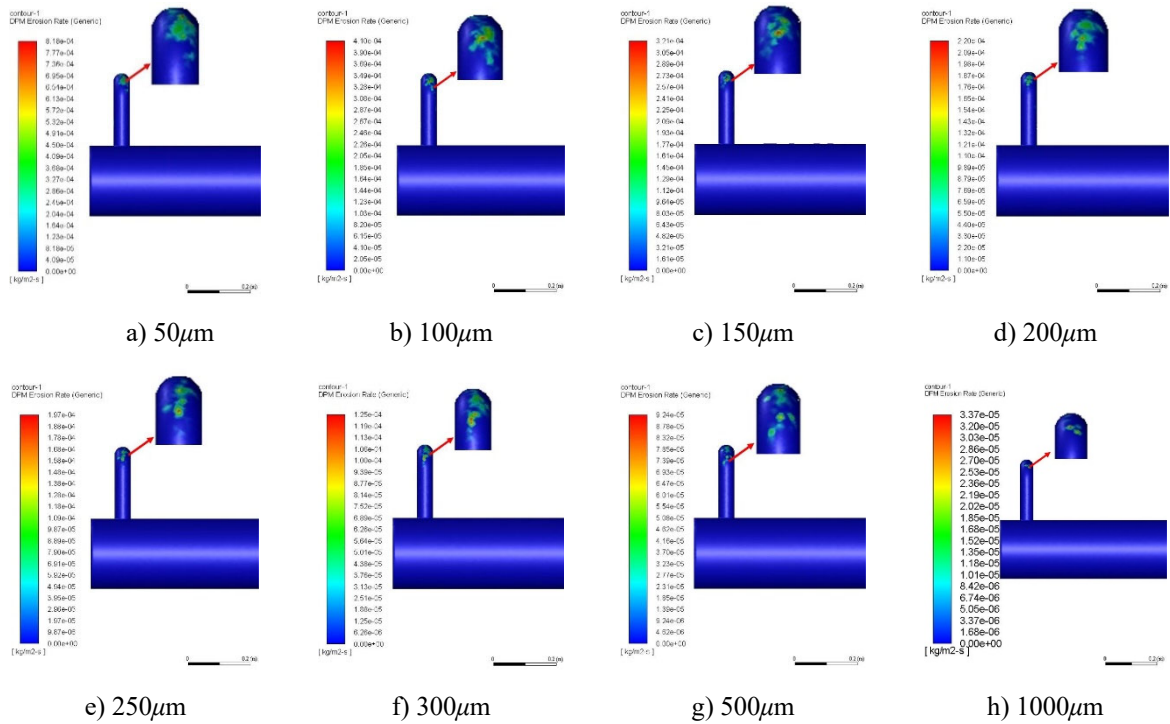


Figure 14. Effect of particle diameter on erosion rate

It can be seen from figure 15 that as the particle diameter increases, the maximum erosion rate of the pipeline decreases, and gradually slows down and tends to be stable. Due to the small particle size of the particles, the contact surface is smaller when colliding with the pipeline, so the force is greater and the erosion rate is greater. From the diagram, it can be seen that the overall erosion rate decreases with the increase of particle size. However, the erosion rate increases

under the two working conditions when the particle size is between $50\mu\text{m}$ and $100\mu\text{m}$. After more than $100\mu\text{m}$, the erosion rate decreases with the increase of particle size, and the maximum erosion rate under gas-solid two-phase is smaller than that of gas-liquid-solid three-phase. The change trend of the two is consistent, but the difference between the two is not significant.

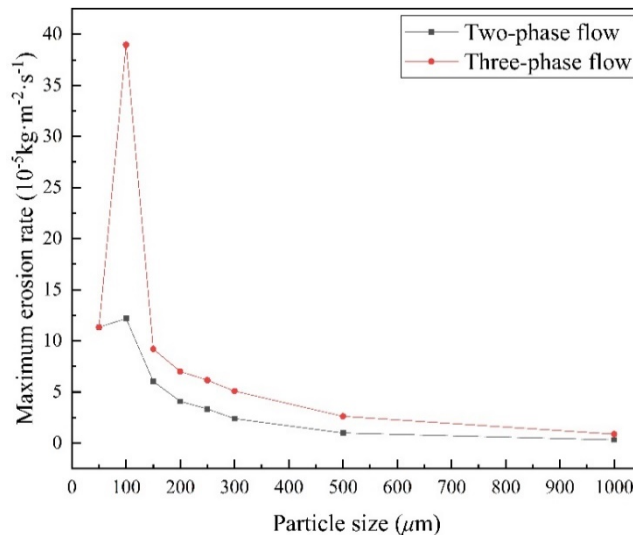


Figure 15. Relationship between particle diameter and maximum erosion rate of pipeline

4.5. The effect of curvature-to-diameter ratio on erosion rate

The influence of the bending diameter ratio at the elbow on the maximum erosion rate was studied. The diameter of the pipe was set to 219mm , the diameter of the vent pipe was set to 50mm , the diameter of the solid particle was set to $100\mu\text{m}$,

the incident velocity was set to 10 m/s , and the mass flow rate was set to 0.2 kg/s . The ratio of bending diameter is set to 1, 2, 3 and 4 respectively. When calculating the influence of the bend diameter ratio on the erosion rate of the pipeline, the above bend diameter ratio parameters are changed in turn.

Figure 16 describes the erosion cloud diagram and particle trajectory of gas-liquid-solid three-phase flow pipeline with

different bending diameter ratios. Obviously, with the increase of the bending diameter ratio, the corner transition radius of the pipeline gradually becomes larger and smoother. Through the particle trajectory in the tube, it can be seen that in the model with a small bending diameter ratio, the particles are more concentrated in the fixed area of the elbow. With the

increase of the bending diameter ratio, the trajectory of the contact between the particles and the bending angle is longer. The effect of this particle trajectory is the reduction of the maximum erosion rate, but the erosion trace changes from a fixed concentrated area to a dispersed area along the elbow.

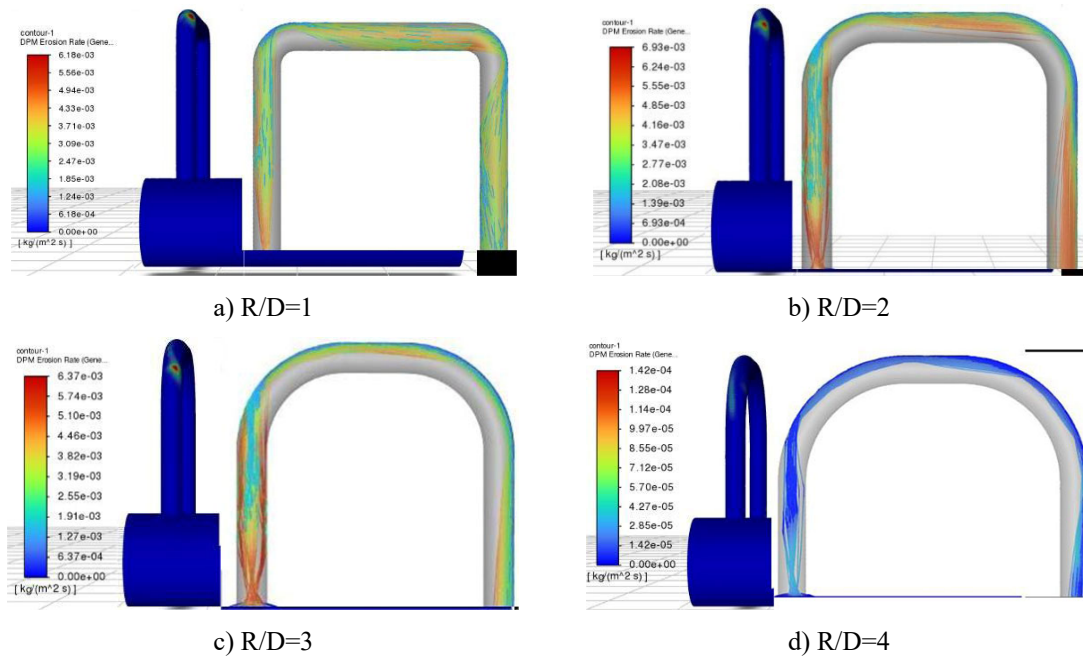


Figure 16. The erosion rate cloud diagram of pipeline wall under different bending diameter ratio

As the bending diameter ratio increases, the erosion rate decreases, as shown in figure 17. When the bend diameter ratio of the pipe elbow changes from 1 to 2, the maximum erosion rate decreases rapidly; when the bending diameter ratio changes from 2 to 4, the maximum erosion rate decreases slowly. Comparing the change trend of the erosion rate curve of the two-phase flow and the three-phase flow, the change trend of the erosion rate of the two working conditions

is basically the same. The erosion rate of the three-phase flow is always greater than that of the two-phase flow. This is because the viscosity of the gas phase is small, and the effect of increasing the velocity of the solid particles is not obvious. The viscosity of the liquid phase in the fluid is large, which affects the movement of the solid particles and increases the kinetic energy of the solid particles.

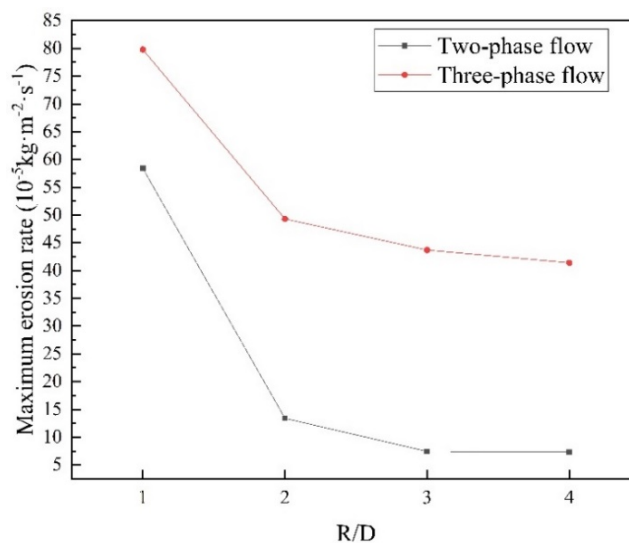


Figure 17. The relationship curve between the maximum erosion rate of the pipeline and the bending diameter ratio

4.6. Effect of pipe diameter on erosion rate

The particle incident velocity is set to 10m/s, the diameter is $100\mu\text{m}$, and the bending diameter ratio is 2. The inner

diameter of the pipe (30mm, 50mm, 70mm, 90mm, 110mm) is changed in turn, and the erosion results of the pipe diameter of 30mm, 70mm and 110mm are given, as shown in figure 18.

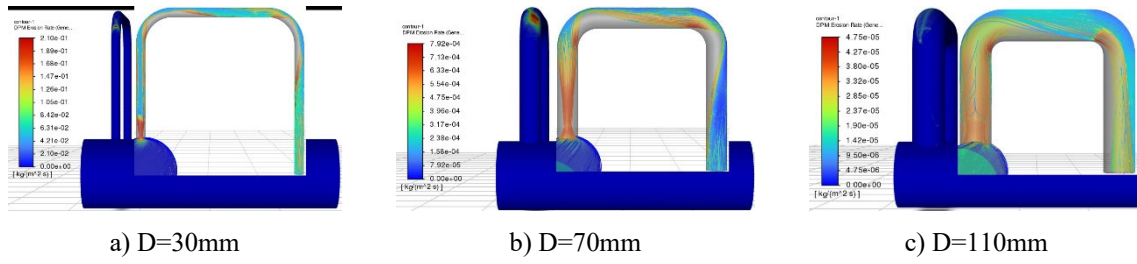


Figure 18. The erosion rate cloud diagram of pipeline wall under different pipe diameters

According to the erosion results, it is not difficult to see that under the condition that other influencing factors remain unchanged, when the pipe diameter is small, the erosion on the pipe wall is more concentrated and the erosion effect is more obvious. This is because when the mass flow rate is constant, the diameter of the pipe is small, and the sand particles will collide with the pipe wall more intensively when passing through the elbow; as the pipe diameter increases, the pipe space increases, and the sand particles are more dispersed when they collide with the wall. With the increase of pipe diameter, the maximum erosion area gradually disappears, which shows that increasing the pipe diameter can effectively prevent the destruction of a certain area of the pipeline due to erosion concentration.

Figure 19 shows the curve of the maximum erosion rate

under two-phase flow and three-phase flow by changing the pipe diameter. On the whole trend, with the increase of pipe diameter, the maximum erosion rate decreases. When the pipe diameter increases from 30mm to 50mm, the maximum erosion rate decreases rapidly. When the pipe diameter exceeds 50mm, the maximum erosion rate hardly changes. This shows that in the small pipe diameter, the change of pipe diameter has obvious influence on the erosion rate, and in the large pipe diameter, the change of pipe diameter has little effect on the change of erosion rate. It can also be seen from the figure that the erosion rate curves of two-phase flow and gas-liquid-solid three-phase flow are basically the same, and the erosion rate of three-phase flow in the presence of liquid phase is greater than that of two-phase flow.

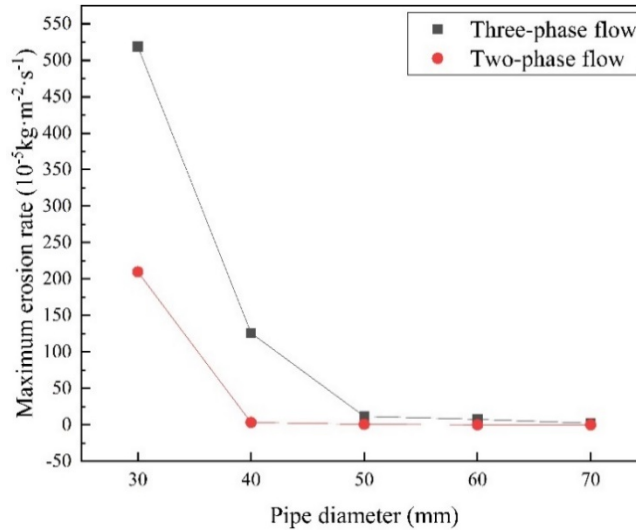


Figure 19. The relationship between the maximum erosion rate and the diameter of the pipe.

5. Correlation Analysis of Influencing Factors of Erosion Rate

The grey correlation degree method is used to analyze the correlation degree between the maximum erosion rate of the pipeline and the diameter, bending diameter ratio, flow rate, particle diameter, particle mass flow rate and other factors in the numerical simulation calculation, and the influence degree of the above influencing factors on the maximum erosion rate of the pipeline can be judged.

The mean value of the correlation coefficient between each index and the corresponding elements of the reference sequence is calculated to reflect the correlation between each evaluation object and the reference sequence:

$$r_i = \frac{1}{m} \sum_{k=1}^m \xi_i(k) \quad (6)$$

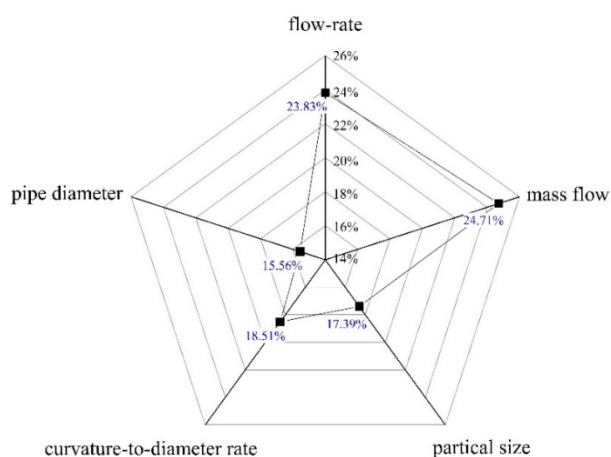
Where: m is the number of indicators; $\xi_i(k)$ is the correlation coefficient; $k=1, 2, \dots, m$.

The above data are brought into the above formula to calculate the correlation coefficient of each influencing factor on the erosion rate, as shown in Table 2. There is a large difference in the values obtained by each factor, indicating that the influence of each factor on the erosion rate is large, and $r_2 > r_1 > r_4 > r_3 > r_5$.

Table 2. Correlation coefficient of each influencing factor

influencing factor	flow rate	mass flow	partical size	curvature-to-diameter rate	pipe diameter
r	0.7327	0.7596	0.5346	0.5689	0.4784

Under the premise of only considering the above factors, it can be seen from figure 20 that the influence of flow rate and mass flow rate on erosion rate is the closest, and both exceed 20%, while the influence of particle size, bending diameter ratio and pipe diameter on erosion rate is close, all less than 20%. It can be known from the calculation results of the correlation degree that the mass flow rate of the particles has the greatest influence on the erosion rate, followed by the flow rate, and the influence of the fluid in the pipeline on the erosion rate exceeds 65%, while the influence of the pipeline structure on the erosion rate is less than 35%. This is because with the increase of flow rate and mass flow rate, the fluid carries more kinetic energy to impact the pipeline, and the particle size affects the flow resistance of the fluid more, so the influence on the erosion rate is smaller than that of flow rate and mass flow rate.

**Figure 20.** Correlation between parameters and erosion rate of pipeline elbow

6. Results and Discussion

Based on the finite element software, the mesh independence of the U-shaped tube was verified. The flow field in the pipeline under the condition of gas-solid two-phase flow was analyzed by computational fluid dynamics. The influence of particle velocity, mass flow rate, particle diameter, bending diameter ratio and pipe diameter on the change of pipeline erosion rate and the location of maximum erosion are analyzed. Finally, according to the erosion calculation results under various factors and the correlation analysis of the influencing factors of erosion rate, the influence degree of each factor on erosion is obtained. The main conclusions are as follows:

(1) When $V=5\text{m/s}$, particle size $100\mu\text{m}$, 0.1kg/s , two-phase flow and gas-liquid-solid three-phase flow with liquid phase volume fraction of 10%, the three-phase has more obvious turbulence intensity change at the elbow than the two-phase action, and the turbulence of the outer arc of the bending diameter is larger than that of the inner arc. The change of pressure and flow velocity in the tube is more obvious than that of gas-liquid-solid three-phase, and there is a greater difference in the same cross section at the elbow.

(2) When other conditions are the same, the erosion rate of the gas-liquid-solid three-phase flow with a liquid phase

volume fraction of 10% is greater than that of the two phases. The flow rate and particle diameter have no obvious effect on the change of the two, but the mass flow rate has a great influence on the erosion rate of the three-phase flow.

(3) Under the conditions of $V=5\text{m/s}$, particle size 100 and 0.1kg/s , in three-phase flow with different liquid volume fractions, the erosion rate increases with the increase of volume fraction when the volume fraction is less than 6%, but decreases when the volume fraction is more than 6%.

Declarations

Ethics approval and consent to participate
Not applicable.

Consent for publication

All the authors have agreed to publish this article.

Availability of data and materials

All materials and data used should be available at Southwest Petroleum University. The datasets used and/or analyzed during the current study are available from the corresponding author on reasonable request.

Competing interests

The corresponding author states that there is no conflict of interest.

Funding

Funded by the author.

Authors' contributions

YC helped with the writing of the manuscript, provided technical guidance, and was a major contributor in writing the manuscript. ZZ collected data, wrote, edited, and translated the manuscript; DYM and JJT provided guidance on manuscripts, and provided guidance and polishing of the manuscript's language.

All authors have read and approved the manuscript.

Acknowledgements

Not applicable.

References

- [1] Nan Lin, Hui Huang, Shili Li, Honglian Ma, Yang Li (2020) Numerical simulation of erosion wear of pipeline elbow in shale gas gathering station. *Sci. Technol. Eng.* 20: 8543-8549. (in Chinese) DOI: 10.3969/j.issn.1671-1815.2020.21.017
- [2] Subhash N.Shah, Samyak Jain (2008) Coiled tubing erosion during hydraulic fracturing slurry flow. *Wear* 264: 279-290. DOI: 10.1016/j.wear.2007.03.016.
- [3] B. Onen, Y. Yildiran, E. Avcu, A. Cinar (2015) Investigation of the effects of erosion test parameters on the particle impingement velocity by using CFD analysis. *Acta Phys. Pol. A* 127: 1225-1229. DOI: 10.12693/APhysPolA.127.1225.

- [4] V. Singh, S. Kumar, S. K. Mohapatra (2019) Modeling of Erosion Wear of Sand Water Slurry Flow through Pipe Bend using CFD. *J. of Appl. Fluid Mech.* 12: 679-687. DOI: 10.29252/jafm.12.03.29199.
- [5] Zhang Jixin, Kang Jian, Fan Jianchun, Gao Jiancun (2016) Research on erosion wear of high-pressure pipes during hydraulic fracturing slurry flow. *J. Loss Prev. Process Ind.* 43: 438-448. DOI: 10.1016/j.jlp.2016.07.008.
- [6] A. Costa, R. Nara (2020) Computational Fluid Dynamics Erosion Investigation Using Single Objective Adjoint Shape Optimization. *J. Pipeline Syst. Eng. Pract.* 11: 6060001(1-8). DOI: 10.1061/(ASCE)PS.1949-1204.0000468.
- [7] Singh Jashanpreet, Singh Jatinder Pal, Singh Mandeep, Szala Miroslaw (2019) Computational analysis of solid particle-erosion produced by bottom ash slurry in 90° elbow. *MATEC Web Conf.* 252: 4008. DOI: 10.1051/mateconf/201925204008.
- [8] Mikilkumar B. Gandhi, Rupa Vuthaluru, Hari Babu Vuthaluru, David H. French, Kalpit Shah (2012) CFD based prediction of erosion rate in large scale wall-fired boiler. *Appl. Therm. Eng.* 42: 90-100. DOI: 10.1016/j.applthermaleng.2012.03.015.
- [9] Waclaw Wojnar (2013) Erosion of heat exchangers due to sootblowing. *Eng. Failure Anal.* 33: 473-489. DOI: 10.1016/j.engfailanal.2013.06.026.
- [10] Jincheng Hu, Rong Li, Deng Li, Yi Hu, Zhen Liu, Xiaochuan Wang (2022) Numerical simulation of erosion wear of fracturing pump valve. *Surf. Technol.* 51: 225-232. (in Chinese) DOI: 10.16490/j.cnki.issn.1001-3660.2022.08.018.
- [11] Fucheng Deng, Bin Huang, Biao Yin, Xiaosen Li, Xianzhong Yi (2022) Study on erosion of slotted liner in shale gas hydrate exploitation. *J. Cent. South Univ.* 53: 1023-1032. (in Chinese) DOI: 10.11817/j.issn.1672-7207.2022.03.023.
- [12] Kun Ding, Hongcheng Yin, Bingqian Wan, Hao Cheng, Lu Xiang, Jianmin Li (2017) Analysis of particle size to erosion wear of sliding sleeve ball seat based on Fluent software. *AIP Conf. Proc.* 1829: 020024. DOI: 10.1063/1.4979756.
- [13] M. Amara, B.G.N. Muthanna, M. Tahar Abbes, M. Hadj Melianiv (2018) Effect of sand particles on the Erosion-corrosion for a different locations of carbon steel pipe elbow. *Procedia Struct. Integr.* 13: 2137-2142. DOI: 10.1016/j.prostr.2018.12.151.
- [14] OM Parkash, Arvind Kumar, Basant Singh Sikarwar (2021) Computational Erosion Wear Model Validation of Particulate Flow Through Mitre Pipe Bend. *Arabian J. Sci. Eng.* 46: 1-18. DOI: 10.1007/s13369-021-05931-x.
- [15] Jukai Chen, Yueshe Wang, Xiufeng Li, Renyang He, Shuang Han, Yanlin Chen (2015) Erosion prediction of liquid-particle two-phase flow in pipeline elbows via CFD-DEM coupling method. *Powder Technol.* 275: 182-187. DOI: 10.1016/j.powtec.2014.12.057.
- [16] G. Grant and W. Tabakoff (1975) Erosion Prediction in Turbomachinery Resulting from Environmental Solid Particles. *J. Aircr.* 12: 471-478. DOI: 10.2514/3.59826.
- [17] Li Chen, Shi-Ming Ji, Dapeng Tan (2012) Multiple-loop digital control method for a 400-Hz inverter system based on phase feedback. *IEEE Trans. Power Electron.* 28: 408-417. DOI: 10.1109/TPEL.2012.2188043.
- [18] Gujun Chen, Qiangqiang Wang, Shengping He (2019) Assessment of an Eulerian multi-fluid VOF model for simulation of multiphase flow in an industrial Ruhrstahl-Heraeus degasser. *Metall. Res. Technol.* 116: 1-10. DOI: 10.1051/metal/2019049.
- [19] Shiming Ji, Xiaoxing Weng, Dapeng Tan (2012) Analysis method of flow field characteristics of soft abrasive two-phase flow based on two-dimensional model of level set method. *J. Phys.* 61: 010205-010205. (in Chinese) DOI: 10.7498/aps.61.010205.
- [20] Ye Pan, Shiming Ji, Dapeng Tan D, Huiqiang Cao (2020) Cavitation-based soft abrasive flow processing method. *Int. J. Adv. Manuf. Technol.* 109: 2587-2602. DOI: 10.1007/s00170-020-05836-3.
- [21] Mengyun Zhang, Guiyang Ma, Cunlei Li, Zonglin Sun, Huizong Xiao (2017) Comparative Analysis of Erosion Wear of Bend Pipe and Blind Pipe. *China Saf. Prod. Sci. Technol.* 13: 76-81. (in Chinese) DOI: 10.7498/aps.61.010205.